Inorganic Chemistry

Article

pubs.acs.org/IC

From 1D Chain to 3D Framework Uranyl Diphosphonates: Syntheses, Crystal Structures, and Selective Ion Exchange

Weiting Yang,[†] Hong-Yue Wu,[†] Run-Xue Wang,[†] Qing-Jiang Pan,[‡] Zhong-Ming Sun,*[,†] and Hongjie Zhang[†]

[†]State Key Laboratory of Rare Earth Resource Utilization, Changchun Institute of Applied Chemistry, Chinese Academy of Sciences, Changchun, 130022, China

[‡]Key Laboratory of Functional Inorganic Material Chemistry of Education Ministry, School of Chemistry and Materials Science, Heilongjiang University, Harbin 150080, China

Supporting Information

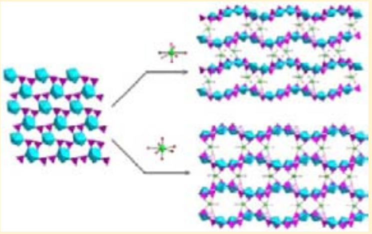

ABSTRACT: In this work, we demonstrate a family of new inorganic−organic hybrid uranyl diphosphonates based on 1-hydroxyethylidenediphosphonic acid (H_4L) linker by using hydrothermal method. These compounds, $(Hbpi)[(UO_2)(H_2O)(HL)]\cdot H_2O$ (**UP-1**), represents 1D structure, $(Hbpi)[(UO_2)(H_2O)(HL)]$ (**UP-2**), $(H_2dib)_{0.5}[(UO_2)(H_2O)(HL)]$ (**UP-3**), and $[(UO_2)(H_2O)(H_2L)]\cdot 2H_2O$ (**UP-4**) feature 2D architectures, $(H_2bipy)\{[(UO_2)(H_2O)]_2[(UO_2)(H_2O)_2](L)_2\}\cdot 2H_2O$ (**UP-5**), and $(H_3O)_2\{[(UO_2)(H_2O)]_3(L)_2\}\cdot 2H_2O$ (**UP-6**) adopt 3D networks (bpi: 1-(biphenyl-4-yl)-1H-imidazole, dib: 1,4-di(1H-imidazol-1-yl)benzene, bipy: 2,2′-bipyridine). Among them, **UP-1**, **UP-2**, **UP-3**, and **UP-4** possess the same structural building unit but with different structures. **UP-5** and **UP-6** feature the same UO_2/L ratio of 3:2 but a different structural building unit. Photoluminescence studies reveal that **UP-5** displays characteristic emissions of uranyl cations. Ion-exchange experiments demonstrate that the H_3O^+ in **UP-6** can be easily and selectively exchanged by monovalent cations including Na^+, K^+, Cs^+, and Ag^+ cations, whereas the framework retains identical as confirmed by single-crystal X-ray diffractions.

■ INTRODUCTION

Uranyl compounds have attracted much attention not only because of the rich structural chemistry[1] but also due to their potential applications in ion exchange,[2] proton conductivity,[3] photochemistry,[4] nonlinear optical materials,[5] catalysis,[6] and especially the tremendous importance of U(VI) in the nuclear energy cycle.[7] The uranyl cation, UO_2^{2+}, favors 4−6 additional coordination in the equatorial plane yielding tetragonal, pentagonal, and hexagonal bipyramidal geometries. Because of the generally inert nature of the two oxo atoms, it is assumed that the formation of 1D or 2D structures is favored, whereas 3D framework would be infrequent. Recent interest in the syntheses of uranyl phosphonates has been raised partly due to the fascinating structural diversity resulting from various coordination modes of the uranium atom and the modification of the organic residues of phosphonates.[8] So far, a large amount of uranyl phosphonates with varied architectures have been documented, including 1D chains[3,9] or tubules,[2,10] 2D layers,[4a,11] and 3D frameworks.[12] This field is burgeoning now with increasingly attractive structural architectures. Of these uranyl phosphonates, organo-templated complex is an important subgroup. Until now, many organo-templated uranyl phosphonates have been reported by using N-heterocyclic compounds,[2a,4a,12d] quaternary amines,[11b] and encapsulated cations as structure-directing agents.[12a] These complexes normally possess anionic frameworks with organic species as the charge compensators.[2a,4a,11b,12d] The organic species play an important structure-directing role in the formation of these hybrid compounds. It is found that one organic template can direct multiple different frameworks under appropriate conditions.[12d] However, multiple different organic templates can also produce the same framework under suitable conditions.[4a,12d] To further elucidate the effect of the organic templates on the resulted structures as well as better understand the structure-directing effect in the syntheses of uranyl phosphonates, we introduce two *N*-heteroaromatic ring-containing molecules, 1-(biphenyl-4-yl)-1H-imidazole (bpi) and 1,4-di(1H-imidazol-1-yl)benzene (dib), as the templates to direct the syntheses of uranyl phosphonates. Neither bpi nor dib has been utilized to synthesize uranyl compounds.

The ion-exchange property of uranium materials has been widely investigated during the past decade.[5a,13−18] Using framework uranium materials as promising hosts for the long-term storage of radionuclides present in used nuclear fuel is advantageous and would be a potential peaceful application of depleted uranium.[13,14] Early studies on the ion exchange of uranium-containing compounds demonstrated the dominance of inorganic uranyl phosphates,[5a,13,15] iodate,[16] and molybdates,[17] as well as organo-templated uranium(IV) fluorides.[14,18] The key feature in common of these materials is that their instability and their preference to rearrange into other condensed compounds upon exposure to metal cations in aqueous solution have limited their application as an ion

Received: June 4, 2012
Published: October 24, 2012

dx.doi.org/10.1021/ic301183h | *Inorg. Chem.* 2012, 51, 11458−11465

exchanger.[5a,9a,10b,13a] However, the confirmation of the ion exchange could be determined by elemental analyses and ion-selective electrodes rather than single-crystal X-ray diffraction (XRD) due to the destroyed crystallinity.[13c,16] It is remarkable that recently Albrecht-Schmitt et al. reported nanotubular uranyl phenylphosphonates CsUbbp-1, CsUbpbp-1 and RbUbpbp-1 for ion exchange, whose structures remain unchanged upon ion exchange.[2] To the best of our knowledge, 3D uranyl phosphonates have not been reported to hold their structural stabilities after ion exchange. More importantly, in all of the above-mentioned compounds, alkali metal cations or protonated organic amine cations were exchanged by other analogous cations. The study of exchanging protons by other ions for uranyl phosphonates is rare.

In this article, we describe the syntheses, structures, and photoluminescence of a series of uranyl diphosphonates $(Hbpi)[(UO_2)(H_2O)(HL)]\cdot H_2O$ (**UP-1**), $(Hbpi)[(UO_2)(H_2O)(HL)]$ (**UP-2**), $(H_2dib)_{0.5}[(UO_2)(H_2O)(HL)]$ (**UP-3**), $[(UO_2)(H_2O)(H_2L)]\cdot 2H_2O$ (**UP-4**), $(H_2bipy)\{[(UO_2)(H_2O)]_2[(UO_2)(H_2O)_2](L)_2\}\cdot 2H_2O$ (**UP-5**), and $(H_3O)_2\{[(UO_2)(H_2O)]_3(L)_2\}\cdot 2H_2O$(**UP-6**). Significantly, the ion-exchange properties of **UP-6** were studied in detail.

■ EXPERIMENTAL SECTION

Materials and Methods. The imidazole-contained organic compounds were obtained from Jinan Camolai Trading Company. All other chemicals were purchased commercially and used without further purification. Energy Disperse Spectroscopy (EDS) spectra were obtained by using a scanning electron microscope (Hitachi S-4800) equipped with a Bruker AXS XFlash detector 4010. The All IR measurements were obtained using a Bruker TENSOR 27 Fourier Transform Infrared Spectrometer. Samples were diluted with spectroscopic KBr and pressed into a pellet. Scans were run over the range 400−4000 cm^{-1}. The photoluminescence (PL) emission spectra were performed on a Hitachi F-4500 spectrophotometer equipped with a 150 W xenon lamp as the excitation source. The photomultiplier tube (PMT) voltage was 700 V, the scan speed was 1200 nm min^{-1}, the excitation and the emission slit width were 5.0 and 5.0 nm, respectively. The spectrum results are obtained in state mode and the data acquiring time of each point in the spectrum is 0.05 s.

Caution! Standard procedures for handling radioactive material should be followed, although the uranyl materials used in the lab contained depleted uranium.

A mixture of H_4L aqueous solution (50 wt %), 0.1 M $UO_2(NO_3)_2$ aqueous solution, $(UO_2)(OAc)_2\cdot 2H_2O$ or $Zn(UO_2)(OAc)_4\cdot 7H_2O$, corresponding organic species and deionized water was loaded into a 20 mL Teflon-lined stainless steel autoclave. The autoclave was sealed and heated at 160 °C for 2 to 5 days, and then cooled to room temperature. Yellow crystals were isolated. The structures of H_4L and organic templates are shown in Scheme 1, and the molar ratios of the mixtures and reaction pH values are listed in Table 1.

Ion-Exchange Experiments. Ion-exchange studies were investigated with selected cations, using $LiNO_3$, $NaNO_3$, KNO_3, CsCl, $AgNO_3$, $CaCl_2$, $TbCl_3$, and pyridine. Synthesized **UP-6** single crystals were placed in glass vials (3 mL), and 1 mL of 0.1 M solutions of respective metal salts were added and the vials were then covered. The solutions were placed in room temperature without disturbing for several days. Suitable crystals were picked up and mounted on the X-ray diffractometer for structural determination and subsequently for elemental analysis using EDS.

Scheme 1. Diphosphonate Ligand and the Organic Templates Used in the Syntheses

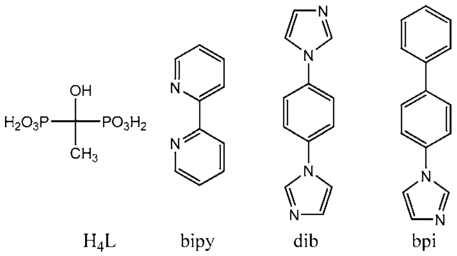

Table 1. Compositions and the pH Values of the Reaction Mixtures

	molar ratios of the reaction mixture	pH[a]
UP-1	0.1 $UO_2(NO_3)_2$: 0.29 H_4L: 0.068 bpi: 503.9 H_2O	2.5, 2.5
UP-2	0.1 $UO_2(NO_3)_2$: 0.29 H_4L: 0.068 bpi: 503.9 H_2O	2.5, 2.5
UP-3	0.1 $UO_2(OAc)_2$: 0.29 H_4L: 0.047 dib: 419.1 H_2O	1.5, 1.0
UP-4	0.1 $UO_2(NO_3)_2$: 0.29 H_4L: 170.5 H_2O	1.5, 1.0
UP-5	0.1 $UO_2(NO_3)_2$: 0.29 H_4L: 0.064 bipy: 503.9 H_2O	1.5, 1.5
UP-6	0.05 $Zn(UO_2)(OAc)_4$: 0.57 H_4L: 173.6 H_2O	1.0, 1.0

[a] The initial and final pH, respectively.

X-ray Structure Determination. Suitable single crystals for **UPs** were selected for single-crystal X-ray diffraction analyses. Crystallographic data were collected at 173 K on a Bruker Apex II CCD diffractometer with graphite monochromated Mo−Kα radiation (λ = 0.71073 Å). Data processing was accomplished with the *SAINT* program.[19] The structure was solved by direct methods and refined on F^2 by full-matrix least-squares using *SHELXTL-97*.[20] Non-hydrogen atoms were refined with anisotropic displacement parameters during the final cycles. All hydrogen atoms of the organic molecule were placed by geometrical considerations and were added to the structure factor calculation. A summary of the crystallographic data for these complexes is listed in Table 2, and the selected bonds and angles are listed in Table S1. Further details of the crystal structure investigation may be obtained from the Cambridge Crystallographic Data Centre on quoting numbers. CCDC 880854−880857, 880861 (**UP-1** to **UP-5**), 857608−857612 (**UP-6**, **6Na**, **6K**, **6Cs**, **6Ag**).

■ RESULTS AND DISCUSSION

Syntheses. All of these **UPs** were prepared using H_4L as ligand under hydrothermal condition. As shown in Table 1, in absence of organic templates, uranyl nitrate led to the layered structure of **UP-4**. When using zinc uranyl acetate instead of uranyl nitrate, 3D framework **UP-6** was formed. It is interesting that the Zn^{2+} was not coordinated to the framework, but the slow release of uranyl ions by uranyl zinc acetate ionization are crucial for the formation of **UP-6**. When adding the second organic compounds as the templates, various structures are produced. The organic template bpi directed the synthesis of **UP-2**, as well as **UP-1** as the minor phase in the same condition. The two compounds possess the same molecular formula of the framework but feature different structures. **UP-3** was synthesized using dib as the template, and with uranyl acetate as the uranium source. We also introduced smaller organic species, bipy, as the template, and 3D framework **UP-5** was formed. These results reveal that the second ligands alter the interaction between the uranyl and the phosphonate groups in the reaction, thus resulting in different architectures. Meanwhile, the configuration and the size of the templates, as well as the species of uranium sources both have important effects on the final structures. Except that, considering these syntheses condition, we can conclude that the acidic environment with pH values of 1.0−2.5 is crucial for the crystallization of the title uranyl phosphonates.

IR Characterization. The IR spectra of the title uranyl diphosphonates are shown in Figure S1 of the Supporting Information. The asymmetric and symmetric stretching modes

Table 2. Crystal Data and Structure Refinement for UP-1 to UP-6[a]

	UP-1	UP-2	UP-3	UP-4	UP-5
empirical formula	$H_{22}C_{17}N_2P_2UO_{11}$	$H_{20}C_{17}N_2P_2UO_{10}$	$H_{13}C_8N_2P_2UO_{10}$	$H_{12}C_2P_2UO_{12}$	$H_{29}C_{14}N_2P_4U_3O_{26}$
fw	730.30	712.30	597.16	528.04	1479.27
T (K)	173(2)				
λ (Å)	0.71073				
space group	$P2_1/c$ (No. 14)	$Pbca$ (No. 61)	$Pbca$ (No. 61)	P-1 (No. 2)	$P2_1/c$ (No. 14)
a (Å)	7.1749(4)	13.1907(19)	13.330(5)	9.556(2)	9.6164(10)
b (Å)	11.4055(6)	12.2801(18)	12.346(5)	9.681(2)	18.5742(19)
c (Å)	27.2222(15)	26.322(4)	18.183(7)	13.750(3)	18.0889(19)
α (deg)	90	90	90	72.899(4)	90
β (deg)	96.6810(10)	90	90	71.041(4)	91.280(2)
γ (deg)	90	90	90	89.750(3)	90
V(Å^3)	2212.6(2)	4263.8(11)	2992.3(19)	1143.9(5)	3230.2(6)
Z, ρ_{calcd} (Mg/m^3)	4, 2.180	8, 2.213	8, 2.642	8, 3.031	4, 3.017
μ(Mo Kα) (mm^{-1})	7.543	7.822	11.117	14.525	15.305
R_1 for [$I > 2\sigma(I)$]	0.0411	0.0374	0.0283	0.0475	0.0566,
wR_2	0.1402	0.0865	0.0656	0.1228	0.1273
	UP-6	**UP-6Na**	**UP-6K**	**UP-6Cs**	**UP-6Ag**
empirical formula	$H_{24}C_4P_4U_3O_{27}$	$Na_2H_{18}C_4P_4U_3O_{25}$	$K_{0.96}H_{19.04}C_4P_4U_3O_{27}$	$Cs_{0.28}H_{19.72}C_4P_4U_3O_{27}$	$Ag_{0.42}H_{21.58}C_4P_4U_3O_{29}$
fw	1342.14	1340.08	1371.30	1366.68	1421.10
T (K)	173(2)				
λ (Å)	0.71073				
space group	$Cmc2_1$ (No. 36)	$Cmc2_1$ (No. 36)	$Cmc2_1$ (No. 36)	$Cmc2_1$ (No. 36)	$Cmc2_1$ (No. 36)
a (Å)	18.5715(14)	18.5849(15)	18.4365(11)	18.6630(13)	18.6688(11)
b (Å)	17.9278(13)	17.9529(14)	17.9175(10)	17.8829(12)	17.9109(10)
c (Å)	9.5221(7)	9.5115(7)	9.5296(6)	9.5330(7)	9.4926(6)
α (deg)	90	90	90	90	90
β (deg)	90	90	90	90	90
γ (deg)	90	90	90	90	90
V(Å^3)	3170.3(4)	3173.5(4)	3148.0(3)	3181.6(4)	3174.1(3)
Z, ρ_{calcd} (Mg/m^3)	4, 2.779	4, 2.813	4, 2.881	4, 2.841	4, 2.961
μ(Mo Kα) (mm^{-1})	15.579	15.584	15.815	15.831	15.866
R_1 for [$I > 2\sigma(I)$]	0.0339,	0.0362	0.0349	0.0390	0.0486
wR_2	0.0977	0.0989	0.0937	0.1061	0.1399

[a] $R_1 = \sum(\Delta F/\sum(F_o))$; w$R_2 = (\sum[w(F_o^2 - F_c^2)])/\sum[w(F_o^2)^2]^{1/2}$, $w = 1/\sigma^2(F_o^2)$.

of U═O are observed from 810 to 940 cm^{-1}.[21] The group of peaks around 1000−1200 cm^{-1} is at expected values for symmetric and asymmetric vibrations of C−OH in phosphonate ligand. The bands between 1400−1460 cm^{-1} are due to CH_3 stretching vibrations. The bands locating about 970 cm^{-1} and in the low wavenumber region from 770 to 560 cm^{-1} are dominated by the O−P−O bending and P−C stretching vibrations. The stretching vibrations of H_2O and OH are indicated around 1640 and 3500 cm^{-1}. It is clearly that the spectra of **UP-1**, **UP-2**, **UP-3**, and **UP-5** exhibit additional vibration peaks around 1340 (C−N), 1500 (C═C), 1580 (C═C), 3120−3160 (C−H) cm^{-1} compared to **UP-4** and **UP-6**, which are attributed to the stretching vibrations of the organic aromatic species.

Structure of (Hbpi)[$(UO_2)(H_2O)(HL)$]·H_2O (UP-1). **UP-1** features the anionic [$(UO_2)(H_2O)(HL)$]$_n$ chain (Figure 1). The protonated organic template bpi, which locates between the chains, interacts with the chains by hydrogen bonds and further stabilizes the structure (N(2)−H···O(4), 2.959 Å). As shown in Figure 1, the chain of **UP-1** comprises the trimeric cluster as its structural building unit (SBU), which is formed by one UO_7 pentagonal bipyramid and two PO_3C tetrahedra. The U atom exists in seven coordinated environment including two linear uranyl oxygen atoms (O═U═O, 179.5(3)°; U═O, 1.760(6) and 1.781(6) Å), four planar μ_2-O atoms from two L ligand (U−O, 2.301(6)−2.366(6) Å), and one aqua ligand (U−O, 2.453(8) Å). The P(1) and P(2) atoms in phosphonate group are all tetrahedrally coordinated by two μ_2-O atoms and one C atom, leaving a terminal O and OH group respectively based on the P−O band length (P(1)−O(9), 1.516(6) Å; P(2)−O(8), 1.548(6) Å). As a result, both the phosphonate ligand and bpi are protonated to keep the charge balance.

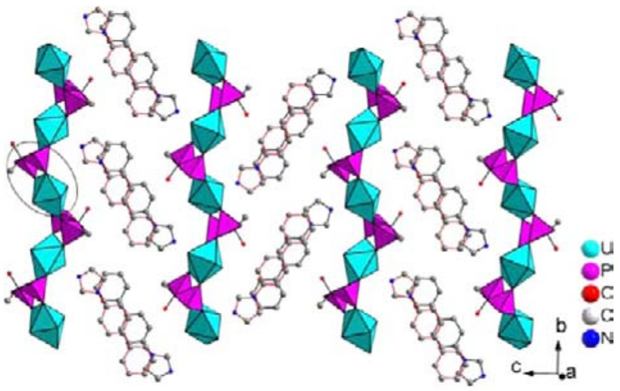

Figure 1. Linear structure of **UP-1** and its SBU in highlight.

Structure of (Hbpi)[$(UO_2)(H_2O)(HL)$] (UP-2) and (H_2dib)$_{0.5}$[$(UO_2)(H_2O)(HL)$] (UP-3). **UP-2** and **UP-3** are isostructural and possess layered architectures (Figure 2a). The layers stack in the AA sequence parallel to the *ac* plane and comprise the same trimeric SBU as in **UP-1**. The protonated organic species bpi and dib exist between the layers of **UP-2** and **UP-3**, respectively and have hydrogen bonds with the layers to stabilize the structures (N(2)−H···O(9), 2.715 Å for **UP-2**; and N(2)−H···O(8), 2.698 Å for **UP-3**). Because of the different template effect, the layers in **UP-2** and **UP-3** exhibit some different degrees of distortion, and different interlayer distance, which are 7.3 Å and 3.7 Å for **UP-2** and **UP-3**, respectively (Figure 2b,c).

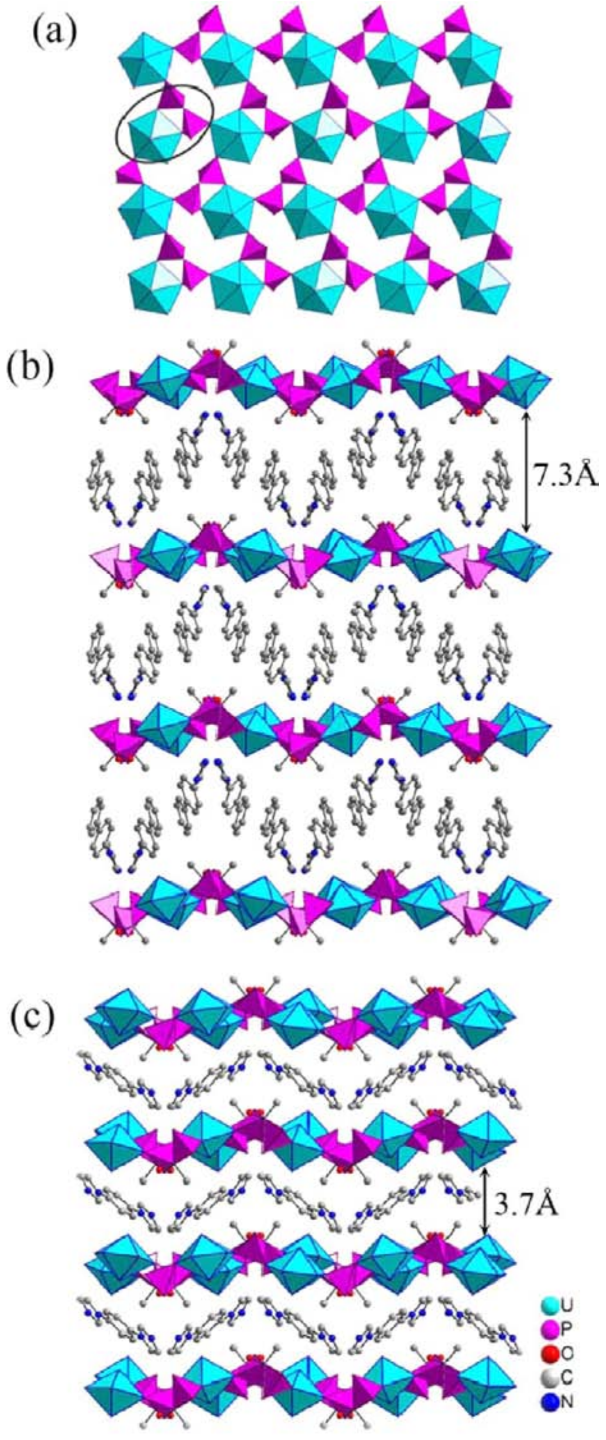

Figure 2. Layer in **UP-2** and **UP-3** and its SBU in highlight (a), the organic species bpi and dib locate between the layers of **UP-2** (b), and **UP-3** (c) respectively viewed along the *b* axis.

Structure of [$(UO_2)(H_2O)(H_2L)$]·$2H_2O$ (UP-4). **UP-4** comprises a layer viewed along the [010] direction (Figure 3a). Such layers stack in a sequence of A, −A to form a double layer unit. Between the double layers, water molecules interact with them though strong hydrogen bonds (Ow···O, 2.544−3.036 Å). As shown in Figure 3b, the layer of **UP-4** also features a trimeric cluster as its SBU formed by one UO_7 pentagonal bipyramid and one H_2L group. The asymmetric unit of **UP-4** contains two uranyl cations and two H_2L groups. Equatorially, the uranium atoms are five coordinated to four μ_2-O atoms from three H_2L groups and one aqua ligand (U−O, 2.335(8)-2.455(8) Å), leaving two axial coordinated oxygen atoms with an average U═O bond distance of 1.756(5) Å.

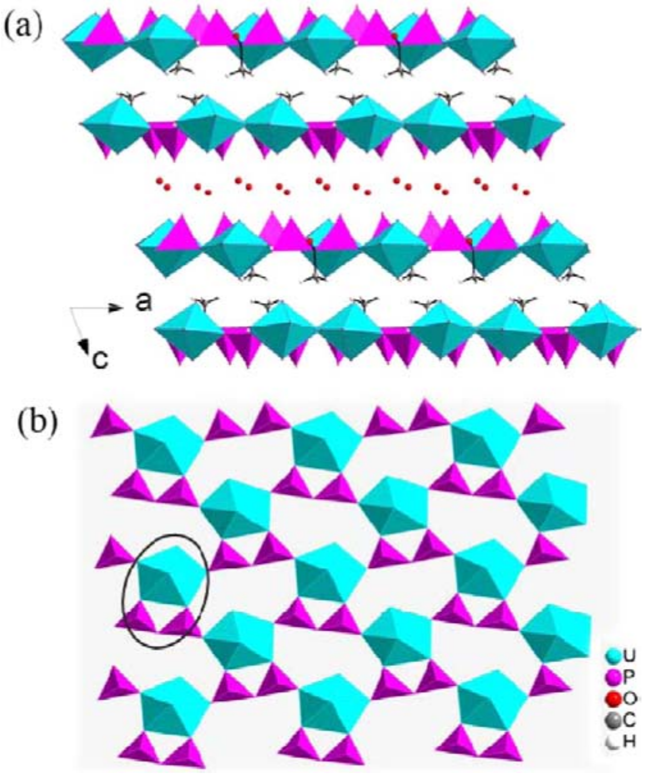

Figure 3. (a) Layers are stacked in a sequence of A, −A in **UP-4**, (b) the single layer and its SBU in highlight.

Structure of (H_2bipy){[$(UO_2)(H_2O)$]$_2$[$(UO_2)(H_2O)_2$]-$(L)_2$}·$2H_2O$ (UP-5). The 3D framework of **UP-5** is connected by UO_7pentagonal bipyramids and L groups with elliptic channels along the [100] direction (Figure 4a). The asymmetric unit of **UP-5** contains three uranyl cations and two L groups. U(1) and U(2) atoms are seven connected to four μ_2-O atoms from three phosphonate groups, two terminal oxygen atoms, and one aqua ligand; thus U(1) and U(2) pentagonal bipyramids can be seen as a four-connected node. Whereas U(3) atom is seven connected to three μ_2-O atoms from two phosphonate groups, two axial coordinated oxygen atoms, and two aqua ligands, resulting in U(3) pentagonal bipyramid as a three-connected node. As shown in Figure 4a, the SBU of **UP-5** is heptameric polyhedra formed by three UO_7 pentagonal bipyramids and two L groups. These SBUs are further connected to each other to form the whole framework

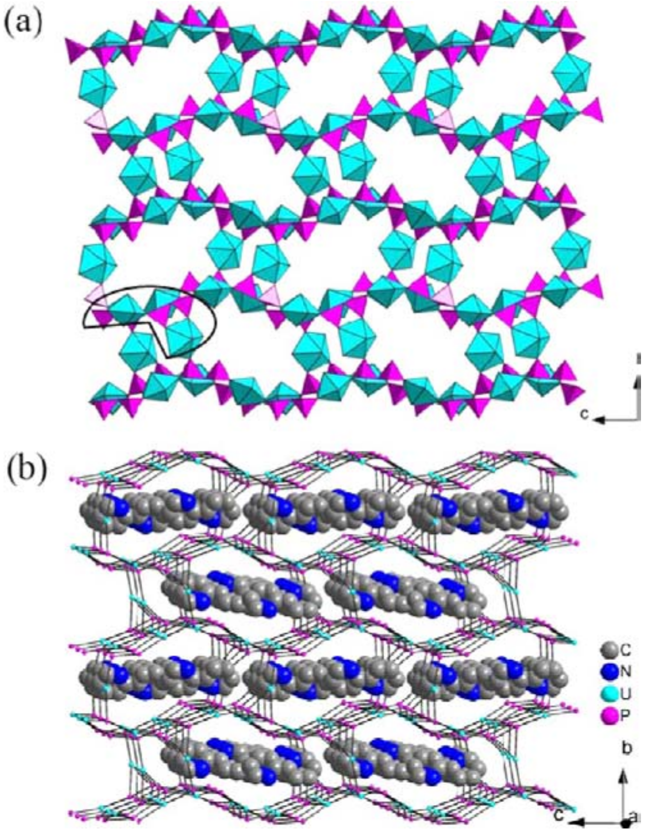

Figure 4. (a) Polyhedral view along the *a* axis of **UP-5** showing the elliptic channels and its SBU in highlight, (b) bipy molecules exist in the channels of **UP-5**.

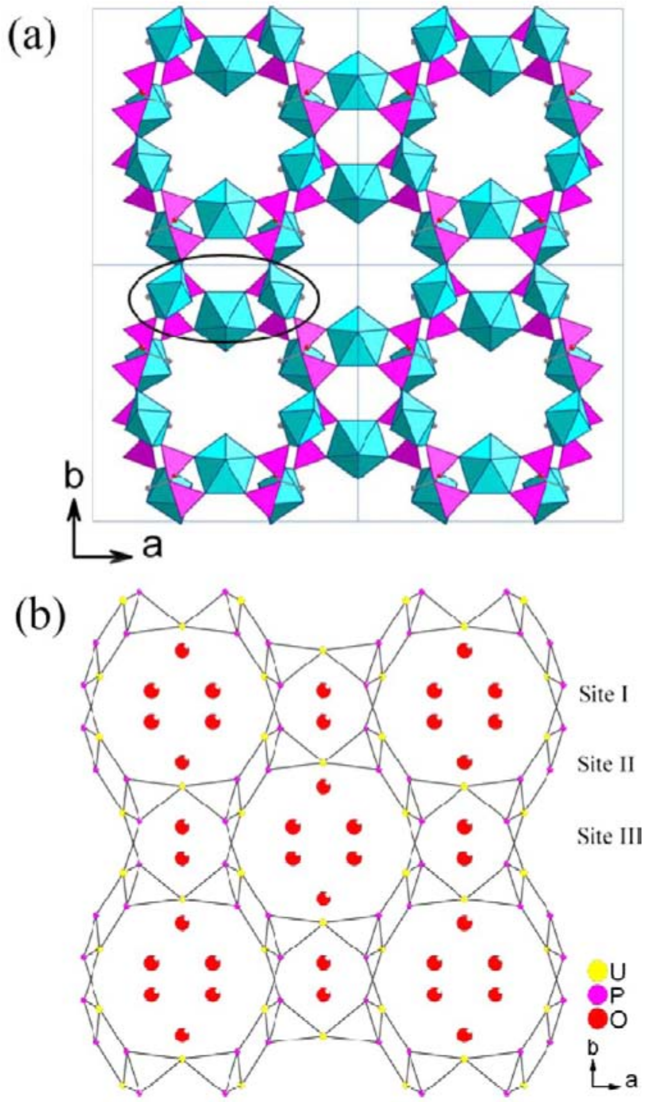

Figure 5. (a) Polyhedral view along the *c* axis of **UP-6** showing the large channels and its SBU in highlight, (b) the locations of water molecules in **UP-6** representing the three different sites.

containing large channels with the aperture of 3.1 × 6.9 Å. Protonated bipy and lattice water locate in the channels to hold the structure (Figure 4b).

Structure of $(H_3O)_2\{[(UO_2)(H_2O)]_3(L)_2\}\cdot 2H_2O$ (UP-6). The structure of **UP-6** adopts a 3D open framework with channels along the *c* axis as shown in Figure 5a. The framework employs heptameric polyhedra formed by three UO_7 pentagonal bipyramids and four PO_3C tetrahedra as its SBU. Such SBUs connect each other through corner sharing to build the whole network with two types of channels. The aperture of the large channels is approximately 5.3 × 6.0 Å, whereas the smaller one is about 2.0 × 2.0 Å. This structure consists of two crystallographically unique uranium centers, U(1) and U(2), both of which are found in the form of uranyl cations with an average U═O bond distance of 1.753(6) Å. The uranyl centers are equatorially five ligated by four oxygen atoms from the phosphonate and one terminal aqua ligand, the average U−O bond to phosphonate is 2.343(3) Å, slightly shorter than the average $U-O_w$ bond (2.493(5) Å). It is notable that the whole framework is anionic and requires protons to compensate the negative charges. There are three potential hydronium ionic sites in this structure based on the single structural analysis (Figure 5b). First is present in the hole of the large channel, which is a general position with O(2w)···O(11) interaction of 2.742(17) Å (site I), second exists besides the uranyl (U(2)) oxo atoms with O(1w)···O(9) distance of 2.23(2) Å (site II), and the last locates in the small channels with O(3w)···O(4) distance of 2.09(2) Å (site III). These water molecules have strong hydrogen bonding interactions with the framework. The hydronium ions, channels and anionic framework of **UP-6** suggest that it may act as a good host material for cationic ion-exchange application. The ion-exchange property of this compound was therefore investigated in detail.

These title compounds are all based on the 1-hydroxyethylidenediphosphonate ligand (L), which is can be seen as the substitution of both hydrogen atoms of the methylene group in methylendiphosphonate by a methyl and a hydroxyl group. However, it is the first time that the L ligand is used for synthesizing uranyl compounds, and the obtained structures are totally different from that synthesized by methydiphosphonate.[22] Insight into these uranyl diphosphonate structures in this work, significantly structural correlations are observed as shown in Table 3. It is noteworthy that **UP-1**, **UP-2**, **UP-3**, and **UP-4** possess very close framework formula but represent three kinds of structures. Interestingly, they all feature the same trimeric cluster formed by one UO_7 pentagonal bipyramid and two PO_3C tetrahedra as their SBU. In **UP-1**, every UO_7pentagonal bipyramid is connected to two L, and every L is linked by two UO_7 pentagonal bipyramids. It means every SBU is further connected by two SBUs to form a linear structure. While in **UP-2**, **UP-3**, and **UP-4**, every UO_7

Table 3. Summary of the Synthesized Compounds, Corresponding Templates, and SBUs

Compound	Space group	Template	SBU	D
UP-1	$P2_1/c$	bpi	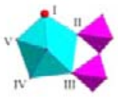	1-D
UP-2	*Pbca*	bpi		2-D
UP-3	*Pbca*	dib		2-D
UP-4	P-1	None	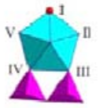	2-D
UP-5	$P2_1/c$	bipy		3-D
UP-6	$Cmc2_1$	None		3-D

pentagonal bipyramid connects three L groups, and every L is bonded to three UO_7 pentagonal bipyramids. Thus, every SBU is further linked to four SBUs, resulting in a layered architecture. Compared **UP-2** with **UP-4**, although every SBU is four-connected, the connection between the UO_7 pentagonal bipyramid and L group are different. For SBU of **UP-2**, the L locates at sites II and III, leaving sites IV and V to link other two phosphonate ligands, whereas in **UP-4** it connects sites III and IV, with sites II and V left (Table 3). It is just because the different connection between and inside the SBUs of these uranyl phosphonates, distinct structures are produced.

It is very significant that 3D framework structures **UP-5** and **UP-6** all comprise the same layer $[(UO_2)(H_2O)(L)]_{2n}$, which is identical to that of **UP-4**. As shown in Figure 6, the layers are stacked in A, −A sequence and further connected by U-centered polyhedra. In **UP-5**, the layers are stacked with a little torsion and joined by three-connected $UO_5(H_2O)_2$ pentagonal bipyramids to construct the 3D network with elliptical channels (monoclinic, $P2_1c$). While in **UP-6**, the layers are linked by four-connected $UO_6(H_2O)$ pentagonal bipyramids to form the 3D structure with circular channels (Orthorhombic, $Cmc2_1$).

Luminescent Properties. All of the synthesized uranyl diphosphonates were studied by photoluminescent spectroscopy. The luminescence of the uranyl recourses, including the H_4L ligand and organic templates, were also investigated (Figures S2−S4). As shown in Figure S4, **UP-1**, **UP-2**, and **UP-3** display fluorescent emission bands with maximum peaks around 434 nm (λ_{ex} = 370 nm), which are very similar to that of free ligands and the organic templates (Figure S3). When excited at the adsorption range of uranyl cation, about 410−440 nm, no emissions are observed. This demonstrates that the emissions are attributed to an intraligand or the organic templates emission state. The luminescent spectra of **UP-4** and **UP-6** are similar to that of **UP-1** (Figure S4) and could originate from the phosphonate ligand. Different from the above-mentioned compounds, **UP-5** exhibits not only the ligand emission but also the uranyl cation emission upon excitation at 370 nm (Figure S4a), which are more evident when excited at 440 nm (Figure S4b). Four prominent peaks, 502, 524, 548, and 574 nm, are clearly observed for **UP-5**, that correspond to the electronic and vibronic transitions $S_{11}-S_{00}$ and $S_{10}-S_{0v}$ (v = 0−4) of uranyl cation. Such spectrum is typical for most uranyl compounds, which exhibit green light centered near 520 nm and often consist of several peaks.[23] Compared to the benchmark compound $UO_2(NO_3)_2{\cdot}6H_2O$ (Figure S2), the luminescence spectrum of **UP-5** exhibits a slight red shift by a value of 14 nm. Looking into the luminescent results of these six complexes, only **UP-5** displays emission of uranyl cation. This is a common phenomenon because not all uranyl compounds exhibit luminescent properties due to their interior nature in bonding, size, and quality of the crystals,[9c,12a,b,f] and so forth. Typical examples were demonstrated by Clearfield et al., who reported two closely related uranyl phenylphosphonate compounds, $[UO_2(HO_3PC_6H_5)_2(H_2O)]_2{\cdot}8H_2O$ and $UO_2(HO_3PC_6H_5)_2(H_2O){\cdot}2H_2O$, in which the former is nonluminescent, whereas the latter is luminescent.[9c]

Ion-Exchange Studies. Monovalent metal ions including Li^+, Na^+, K^+, Cs^+, and Ag^+ cations were first examined. These experiments revealed that **UP-6** is extremely robust in its ion-exchange behavior. Single-crystal XRD analyses for exchanged **UP-6** indicate that all cations except for Li^+ were successfully

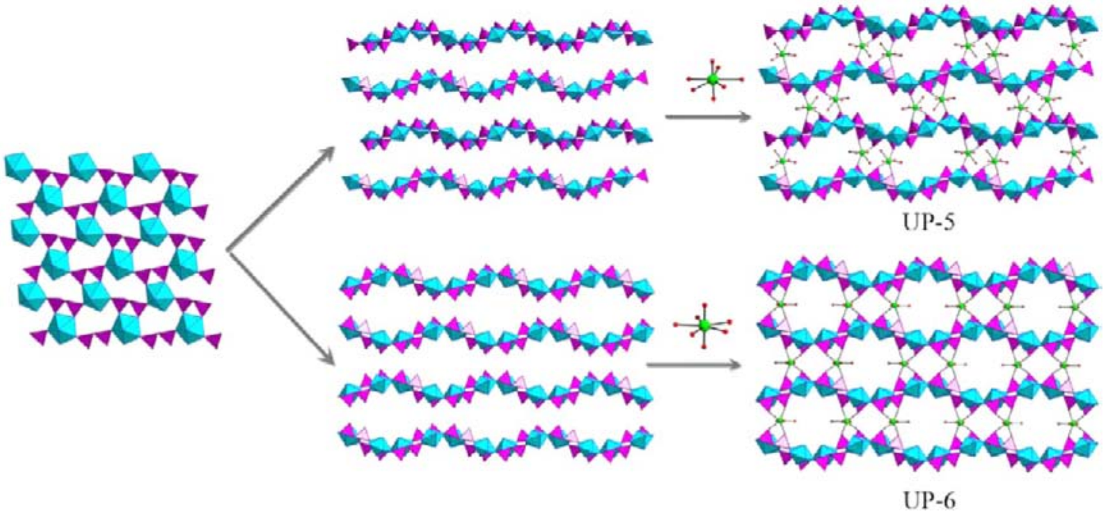

Figure 6. Layers are stacked in A, −A sequence and further connected by three-connected UO_7 pentagonal bipyramids to form **UP-5**, and by four-connected UO_7 pentagonal bipyramids to form **UP-6**, respectively. Color code: blue, U; purple, P; red, O; green, the linkage uranium atoms.

exchanged into the framework. Clear evidence is also indicated by $A^+\cdots O(4)$ distances (site III): O(3w)−O(4) (2.09(2) Å), Na(1)−O(4) (2.98(2) Å), K(1)−O(4) (2.986(10) Å), Cs(1)−O(4) (3.110(13) Å), and Ag(1)−O(4) (2.522(11) Å). It is noted that Na^+ cations are totally exchanged to site I and site III of this framework giving formula of $Na_2\{[(UO_2)(H_2O)]_3(L)_2\}\cdot 2(H_2O)$ (**UP-6Na**). While the other cations are only located in site III by different substitutional contents with formula of $K_{0.96}H_{1.04}\{[(UO_2)(H_2O)]_3(L)_2\}\cdot 4(H_2O)$ (**UP-6K**), $Cs_{0.28}H_{1.72}\{[(UO_2)(H_2O)]_3(L)_2\}\cdot 4(H_2O)$ (**UP-6Cs**), and $Ag_{0.42}H_{1.58}\{[(UO_2)(H_2O)]_3(L)_2\}\cdot 6(H_2O)$ (**UP-6Ag**), respectively (Table 1). In these exchanged structures, Na^+, K^+, Cs^+, and Ag^+ cations are 8-, 9-, 11-, and 5-coordinated by framework oxygen atoms and lattice water molecule, respectively (Figure 7). The detailed bond lengths of these exchanged cations are listed in Table S2. The successful ion exchange for monovalent cations was further confirmed by EDX results shown in Figure 7 and Figure S5. The reason that Li^+ was not exchanged may be due to its comparatively small ionic radii (R_{Li} = 0.76 Å, R_{Na} = 1.39 Å, R_K = 1.64 Å, R_{Cs} = 1.88 Å, R_{Ag} = 1.28 Å). Efforts made to exchange bivalent Ca^{2+} ion, trivalent Tb^{3+} ion, and organic pyridine molecule failed. The ion exchange results indicate that **UP-6** exhibits the selective ion exchange for monovalent cations with proper ionic radii (especially for Na^+), which is related not only to size but also to charge. As far as we know, most of the ion-exchange experiments for framework uranium materials were carried out in highly concentrated solution with stirring and/or heating using one metal ion exchanging for another metal ion, and the crystallinity was too damaged to carry on single-crystal XRD characterization. Alternatively, in **UP-6**, the hydronium ions acted as the exchanger and easily exchanged at room temperature without stirring. This behavior suggests that the hydronium ions in the framework possess strong activity and could be easily exchanged.

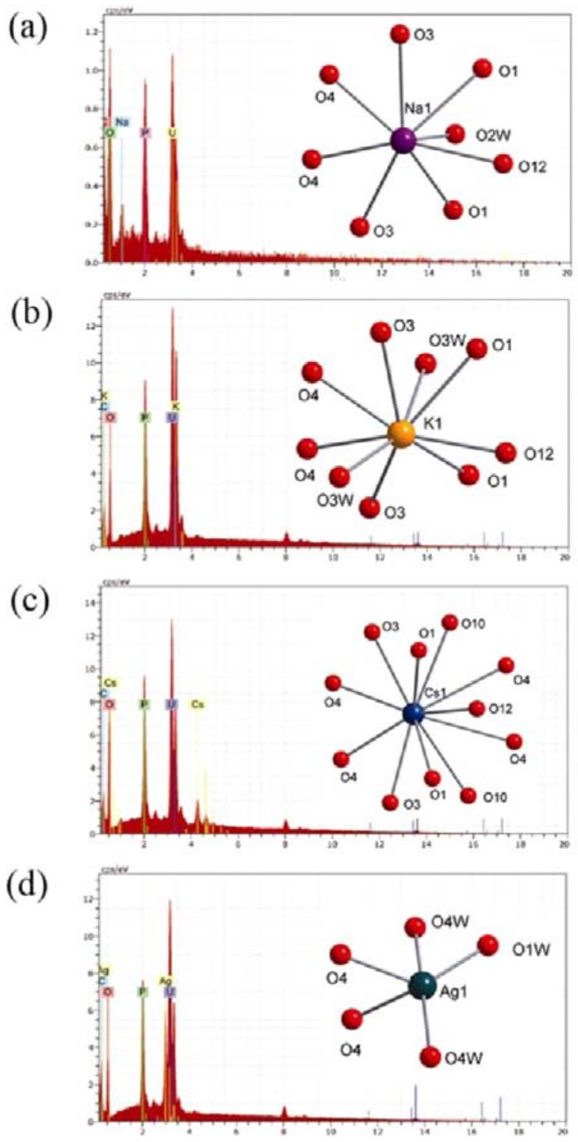

Figure 7. EDX results and the coordinated environments of the Na^+ (a), K^+ (b), Cs^+ (c), and Ag^+ (d) cations in the **UP-6** framework (after ion exchange) showing the interactions with the framework oxygen atoms and water molecules.

■ CONCLUSIONS

In summary, six uranyl diphosphonates with H_4L as the ligand were synthesized by hydrothermal method. Single-crystal analyses reveal that these complex exhibit rich structural variation including 1D, 2D, and 3D architectures. Significantly, these compounds show closely relationship in structures: **UP-1**, **UP-2**, **UP-3**, and **UP-4** possess the same uranyl phosphonate SBU, but with different structures, in which **UP-1** is a linear structure with dpi between the chains, **UP-2** and **UP-3** are layered isostructures with dpi and dib located between the layers, respectively, and **UP-4** is a template-free 2D structure with lattice water molecules holding the layers. **UP-5** and **UP-6** are 3D open frameworks, which can be seen as the **UP-4** layers connected by three-connected and four-connected UO_7 pentagonal bipyramids, respectively. These structure analyses demonstrate that the **UP-4** layer possesses the rich connection diversities and is a candidate for further constructing novel uranyl phosphonates by introducing other transition metals or organic templates.

Among these compounds, **UP-5** exhibits the emission of uranyl cation. Besides, **UP-6**, comprising large channels and H_3O^+ cations, is a good ion exchanger, and some important observations and conclusions were made though ion-exchange studies. First, the framework is fully robust to allow the single crystals to withstand ion exchange without degradation or damage. Second, the hydronium ions exhibit selective ion exchange, which favor to be exchanged by monovalent metal ions with proper ionic radii depending on ionic size as well as charge. Third, the hydronium ions seem to be exchanged more easily than metal ions and protonated organic molecules for uranium compounds in moderate condition. We therefore conclude that hydronium ions in uranyl phosphonates are very active, and selective ion exchange even physicochemical property relationships can be derived from such framework. Future work will be focused on syntheses and characterization of other uranyl phosphonates with different organic templates and exploit the potential peaceful application of depleted uranium.

■ ASSOCIATED CONTENT

Ⓢ Supporting Information

X-ray crystallographic cif files, selected bond lengths and angles, the environments of the different ions in ion-exchanged **UP-6**, the IR spetra, the photoluminescence spectra, the SEM images, and the EDX patterns. This material is available free of charge via the Internet at http://pubs.acs.org.

AUTHOR INFORMATION

Corresponding Author

*E-mail: szm@ciac.jl.cn.

Notes

The authors declare no competing financial interest.

ACKNOWLEDGMENTS

This work was supported by the National Nature Science Foundation of China (No. 21171662), SRF for ROCS (State Education Ministry), Program for New Century Excellent Talents in University (NECT-11-0958) and CIAC startup fund. We thank Dr. En Ma for his valuable discussions.

REFERENCES

(1) (a) Wang, K. X.; Chen, J. S. *Acc. Chem. Res.* **2011**, *44*, 531−540. (b) Ling, J.; Qiu, J.; Sigmon, G. E.; Ward, M.; Szymanowski, J. E. S.; Burns, P. C. *J. Am. Chem. Soc.* **2010**, *132*, 13395−13402. (c) Ok, K. M.; Sung, J.; Hu, G.; Jacobs, R. M. J.; O'Hare, D. *J. Am. Chem. Soc.* **2008**, *130*, 3762−3769. (d) Sigmon, G. E.; Burns, P. C. *J. Am. Chem. Soc.* **2011**, *133*, 9137−9139. (e) Ling, J.; Wallace, C. M.; Szymanowski, J. E. S.; Burns, P. C. *Angew. Chem., Int. Ed.* **2010**, *49*, 7271−7275. (f) Wu, H. Y.; Wang, R. X.; Yang, W. T.; Chen, J. L.; Sun, Z. M.; Li, J.; Zhang, H. J. *Inorg. Chem.* **2012**, *51*, 3103−3107. (g) Mihalcea, I.; Henry, N.; Volkringer, C.; Loiseau, T. *Cryst. Growth Des.* **2012**, *12*, 526−535. (h) Mihalcea, I.; Henry, N.; Clavier, N.; Dacheux, N.; Loiseau, T. *Inorg. Chem.* **2011**, *50*, 6243−6249.

(2) (a) Adelani, P. O.; Albrecht-Schmitt, T. E. *Angew. Chem., Int. Ed.* **2010**, *49*, 8909−8911. (b) Adelani, P. O.; Albrecht-Schmitt, T. E. *Inorg. Chem.* **2011**, *50*, 12184−12191.

(3) Grohol, D.; Subramanian, M. A.; Poojary, D. M.; Clearfield, A. *Inorg. Chem.* **1996**, *35*, 5264−5271.

(4) (a) Knope, K. E.; Cahill, C. L. *Inorg. Chem.* **2009**, *48*, 6845−6851. (b) Jiang, Y. S.; Yu, Z. T.; Liao, Z. L.; Li, G. H.; Chen, J. S. *Polyhedron* **2006**, *25*, 1359−1366.

(5) (a) Ok, K. M.; Baek, J.; Halasyamani, P. S.; O'Hare, D. *Inorg. Chem.* **2006**, *45*, 10207−10214. (b) Wang, S.; Alekseev, E. V.; Ling, J.; Liu, G.; Depmeier, W.; Albrecht-Schmitt, T. E. *Chem. Mater.* **2010**, *22*, 2155−2163.

(6) Liao, Z. L.; Li, G. D.; Bi, M. H.; Chen, J. S. *Inorg. Chem.* **2008**, *47*, 4844−4853.

(7) (a) Ewing, R. C. *Elements* **2006**, *2*, 331−334. (b) Bruno, J.; Ewing, R. C. *Elements* **2006**, *2*, 343−349.

(8) Mao, J. G. *Coord. Chem. Rev.* **2007**, *251*, 1493−1520.

(9) (a) Knope, K. E.; Cahill, C. L. *Eur. J. Inorg. Chem.* **2010**, 1177−1185. (b) Grohol, D.; Gingl, F.; Clearfield, A. *Inorg. Chem.* **1999**, *38*, 751−756. (c) Grohol, D.; Clearfield, A. *J. Am. Chem. Soc.* **1997**, *119*, 4662−4668. (d) Alsobrook, A. N.; Zhan, W.; Albrecht-Schmitt, T. E. *Inorg. Chem.* **2008**, *47*, 5177−5183. (e) Adelani, P. O.; Albrecht-Schmitt, T. E. *Inorg. Chem.* **2010**, *49*, 5701−5705.

(10) (a) Poojary, D. M.; Cabeza, A.; Aranda, M. A. G.; Bruque, S.; Clearfield, A. *Inorg. Chem.* **1996**, *35*, 1468−1473. (b) Aranda, M. A. G.; Cabeza, A.; Bruque, S.; Poojary, D. M.; Clearfield, A. *Inorg. Chem.* **1998**, *37*, 1827−1832. (c) Grohol, D.; Clearfield, A. *J. Am. Chem. Soc.* **1997**, *119*, 9301−9302.

(11) (a) Knope, K. E.; Cahill, C. L. *Inorg. Chem.* **2008**, *47*, 7660−7672. (b) Adelani, P. O.; Oliver, A. G.; Albrecht-Schmitt, T. E. *Cryst. Growth Des.* **2011**, *11*, 1966−1973.

(12) (a) Adelani, P. O.; Albrecht-Schmitt, T. E. *Cryst. Growth Des.* **2011**, *11*, 4227−4237. (b) Adelani, P. O.; Albrecht-Schmitt, T. E. *J. Solid State Chem.* **2011**, *184*, 2368−2373. (c) Adelani, P. O.; Oliver, A. G.; Albrecht-Schmitt, T. E. *Cryst. Growth Des.* **2011**, *11*, 3072−3080. (d) Adelani, P. O.; Albrecht-Schmitt, T. E. *Inorg. Chem.* **2009**, *48*, 2732−2734. (e) Alsobrook, A. N.; Albrecht-Schmitt, T. E. *Inorg. Chem.* **2009**, *48*, 11079−11084. (f) Wu, H. Y.; Yang, W. T.; Sun, Z. M. *Cryst. Growth Des.* **2012**, *12*, 4669−4675.

(13) (a) Ok, K. M.; Doran, M. B.; O'Hare, D. *Dalton Trans.* **2007**, 3325−329. (b) Shvareva, T. Y.; Skanthakumar, S.; Soderholm, L.; Clearfield, A.; Albrecht-Schmitt, T. E. *Chem. Mater.* **2007**, *19*, 132−134. (c) Shvareva, T. Y.; Sullens, T. A.; Shehee, T. C.; Albrecht-Schmitt, T. E. *Inorg. Chem.* **2005**, *44*, 300−305.

(14) (a) Francis, R. J.; Halasyamani, P. S.; O'Hare, D. *Chem. Mater.* **1998**, *10*, 3131−3139. (b) Francis, R. J.; Halasyamani, P. S.; O'Hare, D. *Angew. Chem., Int. Ed.* **1998**, *37*, 2214−2217.

(15) Francis, R. J.; Drewitt, M. J.; Halasyamani, P. S.; Ranganathachar, C.; O'Hare, D.; Clegg, W.; Teat, S. J. *Chem. Commun.* **1998**, 279−280.

(16) Shvareva, T. Y.; Almond, P. M.; Albrecht-Schmitt, T. E. *J. Solid State Chem.* **2005**, *178*, 499−504.

(17) Halasyamani, P. S.; Francis, R, J.; Walker, S. M.; O'Hare, D. *Inorg. Chem.* **1999**, *38*, 271−279.

(18) Walker, S. M.; Halasyamani, P. S.; Allen, S.; O'Hare, D. *J. Am. Chem. Soc.* **1999**, *121*, 10513−10521.

(19) SMART and SAINT (software packages), Siemens Analytical X-ray Instruments, Inc.: Madison, WI, 1996.

(20) SHELXTL Program, version 5.1; Siemens Industrial Automation, Inc.: Madison, WI, 1997.

(21) (a) Bartlett, J. R. *J. Mol. Struct.* **1989**, *193*, 295−300. (b) Frost, R. L.; Cejka, J.; Dickfos, M. J. *Spectrochim. Acta, Part A* **2009**, *71*, 1799−1803.

(22) (a) Nelson, A.-G. D.; Alekseev, E. V.; Ewing, R. C.; Albrecht-Schmitt, T. E. *J. Solid State Chem.* **2012**, *192*, 153−160. (b) Diwu, J.; Albrecht-Schmitt, T. E. *Inorg. Chem.* **2012**, *51*, 4432−4434. (c) Nelson, A.-G. D.; Bray, T. H.; Zhan, W.; Haire, R. G.; Sayler, T. S.; Albrecht-Schmitt, T. E. *Inorg. Chem.* **2008**, *47*, 4945−4951. (d) Knope, K. E.; Cahill, C. L. *Dalton Trans.* **2010**, *39*, 8319−8324.

(23) Liu, G.; Beitz, J. V. In *The Chemistry of the Actinide and Transactinide Elements*; Morss, L. R., Edelstein, N. M., Fuger, J., Eds.; Springer: Heidelberg, 2006; p 2088.